IEEE/CSC & ESAS European Superconductivity News Forum (ESNF), No. 6, October 2008
(ASC Preprint 3EPF01 conforming to IEEE Policy on Electronic Dissemination, Section 8.1.9)

The published version of this manuscript appeared in *IEEE Transactions on Applied Superconductivity* **19**, No. 3, Part 1, 199 - 205 (2009)

Optimization of a low-Tc dc SQUID amplifier with tightly coupled input coils

J. Pleikies, O. Usenko, G. Frossati, and J. Flokstra

***Abstract*— We optimized the design and operation of a low-Tc direct current superconducting quantum interference device (dc SQUID) with an integrated coupling coil of 1.5 µH inductance taking into account typical effects observed for similar devices. Numerical simulations were performed on a model including the capacitance of the Josephson junctions, thermal noise of the integrated shunt- and damping- resistors as well as a complex frequency dependent impedance of the SQUID loop originating from the integrated coils. The experimentally and numerically determined characteristics and sensitivity are in good agreement. A minimum additional coupled energy resolution of 700 ħ and 250 ħ was measured at a temperature of 4.2 K and 1.5 K, respectively.**

***Index Terms*— Circuit simulation, Current sensors, Josephson device noise, SQUIDs.**

I. INTRODUCTION

SQUIDs can not only reach excellent flux-sensitivities [1],[2], in general the amounts of energy that can be detected are very low. This makes them good candidates for precise measurements of any observable that can be converted into a magnetic flux. We concentrate on optimizing such SQUID amplifiers for the readout of the resonant mass gravitational wave antenna MiniGRAIL [3]. Here, a surface displacement of a cooled 1.4 ton heavy sphere is converted by a capacitive transducer to a charging current which then, using a coupling coil, is measured as a magnetic flux in a dc SQUID. To reach the highest sensitivity, a minimum noise at the aimed operation temperature of 20 mK is required in the audio frequency range. The best achieved noise temperature of a comparable sensor corresponds to 50 times the theoretical quantum limit [4]. The noise temperature is dependent on the back-action and the additional noise of the SQUID amplifier. In this paper we do not treat the back-action noise, although we are able to extract it from the numerical model presented here. Instead, we first concentrated on the minimization of the additional noise in our experimental characterization, which strongly correlates to the noise temperature including both noise contributions.

Further, a high coupling factor between the coupling coil and the SQUID inductance is required. The best way to increase the coupling efficiency is to integrate the coil directly on the SQUID. A lot of work was done in several groups on such sensors both experimentally and theoretically [5]-[11]. It turns out that a drawback in integrating the coil on the SQUID washer can be found in introduced parasitic capacitances that influence the dynamics of the SQUID. After all it remains no trivial task to predict the performance of such sensors during the design process. The reasons for this can be found in the nonlinear dynamic behavior of the device. Even the characteristics and sensitivity of standard dc SQUIDs could originally only be explained on the basis of numerical simulations [1]. The integrated coil extends the model to a much higher complexity, which makes it much harder to predict the expected behavior during the design process.

We earlier designed and measured SQUIDs with integrated input coil that strongly deviated [12] from the predictions by standard theory [1],[2]. Especially below 4.2 K we observed distorted and extremely steep flux-to-voltage characteristics [12], which later turned out to be partly hysteretic [13]. In numerical simulations on detailed models of the SQUIDs the characteristics and sensitivity could be reproduced in a good way, revealing that the dynamics are mainly dominated by the integrated coils [13]. The gained experience was now used to perform a new design step for the low-Tc SQUID process at the IPHT Jena [14].

II. DC SQUID AMPLIFIERS

The schematic of a standard dc SQUID with a coupling coil is shown in Fig. 1. This device is forming the basis for measuring electrical currents or voltages or as a magnetometer with an attached pickup coil [15].

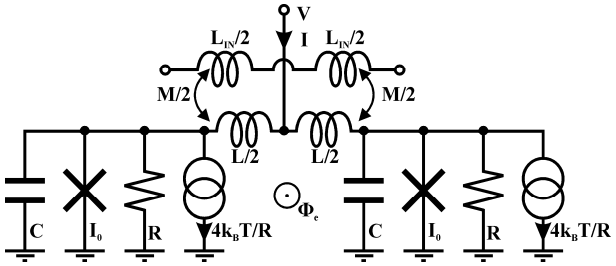

Fig. 1. Schematic of a dc SQUID with coupling coil.

It is useful to directly define some parameters that are widely used for describing SQUIDs [1,2]. The screening-parameter $\beta_L=2\cdot L\cdot I_0/\Phi_0$ is a measure for the coupling of the Josephson junction with critical current I_0 and the SQUID inductance L. Its optimum value, minimizing the additional

Manuscript received August 19, 2008. This work was supported in part by Stichting Technische Wetenschappen (STW).

J. Pleikies, and J. Flokstra are with the Low Temperature division at the Faculty of Science and Technology, University of Twente, P.O. Box 217, 7500 AE Enschede, The Netherlands (phone: +31-53-489-3125; fax: +31-53-489-1099; e-mail: j.pleikies@tnw.utwente.nl).

O. Usenko, and G. Frossati are with the Kamerlingh Onnes Laboratory of the Leiden University, P.O. Box 9504, 2300 RA Leiden, The Netherlands (e-mail: usenko@physics.leidenuniv.nl).

flux noise, is usually given by 1. Φ_0 is the magnetic flux quantum of $2.07 \cdot 10^{-15}$ Wb. The McCumber parameter $\beta_C = 2\pi \cdot I_0 \cdot C \cdot R^2/\Phi_0$ describes the hysteresis of the Josephson junction. Here, values below 1 are required for a non-hysteretic behavior of the Josephson junction. C indicates the capacitance of the Josephson junction and R the externally connected shunt resistor. Finally, the noise parameter $\Gamma = 2\pi \cdot k_B \cdot T \cdot (I_0 \cdot \Phi_0)^{-1}$ relates the influence of thermal noise on the Josephson junction, where $k_B = 1.38 \cdot 10^{-23}$ J/K is the Boltzmann constant and T is the temperature. For typical low-Tc SQUIDs Γ is in the order of 0.05.

The SQUID can be biased with a constant current I and then a voltage with dc value V and a noise power spectral density (PSD) S_V can be measured. Throughout this paper we will use single-sided spectra. Applying an external flux Φ_e, for example by sending a current through the coupling inductance L_{IN}, results in a modulation of the dc voltage with a period of 1 Φ_0. The (additional) flux noise PSD S_Φ of the SQUID is then, depending on the working point,

$$S_\Phi = S_V \cdot (\partial V/\partial \Phi_e)^{-2}. \quad (1)$$

Here, $\partial V/\partial \Phi_e$ denotes the small-signal flux-to-voltage transfer function. The flux noise S_Φ can be directly measured by operating the SQUID in flux-locked loop (FLL) [2], assuming the SQUID is the dominant noise source in the measurement system. To compare different coupled SQUIDs, the noise energy per bandwidth ε referred to the input coil, the coupled energy resolution, is a good figure of merit:

$$\varepsilon = S_\Phi \cdot L_{IN} \cdot M^{-2}/2. \quad (2)$$

Here, M is the mutual inductance between the SQUID inductance L and the coupling inductance L_{IN}.

Using numerical simulations, Tesche and Clarke first determined the sensitivity of the dc SQUID [1]. Their approximation formulas for the white noise region [1],[2]

$$\partial V/\partial \Phi_e \approx R/L,\ S_V \approx 16 \cdot k_B \cdot T \cdot R \text{ and } S_\Phi \approx 16 \cdot k_B \cdot T \cdot L^2/R \quad (3)$$

are widely used for dc SQUIDs with β_L in the order of 1, β_C lower than 1, and Γ much smaller than 1.

III. Simulations on SQUIDs

In contrast to the classical numerical calculations on SQUIDs [1], we did not directly solve the Langevin equations. We used the SPICE-based electrical circuit simulator JSIM [16] which includes the resistively, capacitively shunted model of Josephson junctions. The extension with noise sources [16] allows to include the thermal noise of resistors. The advantage of using a circuit simulator is that the complexity of the circuit under investigation can be extended more easily.

The setup used to characterize SQUIDs within JSIM is schematically shown in Fig. 2. The SQUID is biased at the desired bias current and flux. The maximum simulation time step is chosen a factor of 20 smaller than a period of the plasma frequency of the Josephson junction $I_0^{1/2} \cdot (2\pi \cdot \Phi_0 \cdot C)^{-1/2}$. At the rate of the maximum time steps, also random currents are induced by attached noise sources.

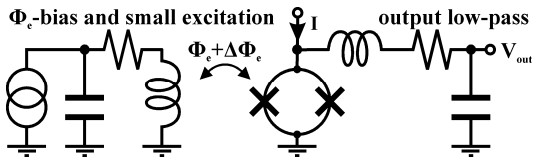

Fig. 2. Schematic of the circuit simulated in JSIM for characterizing SQUIDs. No noise sources are attached to the resistors shown here, which are only used to reduce the quality factor of the two low-pass filters to 1.

Via a low-pass filter the output signal is restricted to the low frequency white noise. Its parameters are chosen such that there is no serious impedance matching with the SQUID at practical frequencies. The time constant of the readout is chosen bigger than the slowest time constant of the sensor. For a SQUID with a many-turn integrated input coil this corresponds to the time-constant of the resonance of the input coil. For a standard SQUID a cutoff frequency of $2\pi \cdot I_0 \cdot R/(100 \cdot \Phi_0)$ proved to be practical. The variance of the filtered voltage var(V_{out}) is then directly related to the effective bandwidth of the low-pass filter and the noise level. Assuming white noise and a second order low-pass filter, as used in our case, with a quality factor $Q_{LP} = R_{LP}^{-1} \cdot (L_{LP}/C_{LP})^{1/2} = 1$ and a cutoff frequency of the low-pass $f_{LP} = (2\pi)^{-1}(L_{LP} \cdot C_{LP})^{-1/2}$, the white noise PSD $S_{V,out}$ is calculated by

$$S_{V,out} = \mathrm{var}(V_{out})/(f_{LP} \cdot \pi/2). \quad (4)$$

To determine the flux sensitivity S_Φ, a small flux excitation is applied during the same simulation by the left auxiliary circuit shown in Fig. 2. Also this circuit is chosen to heavily mismatch with the impedance of the SQUID. By measuring the excitation flux, the covariance cov(V_{out},Φ_e) between the output voltage and the excitation can be determined. The

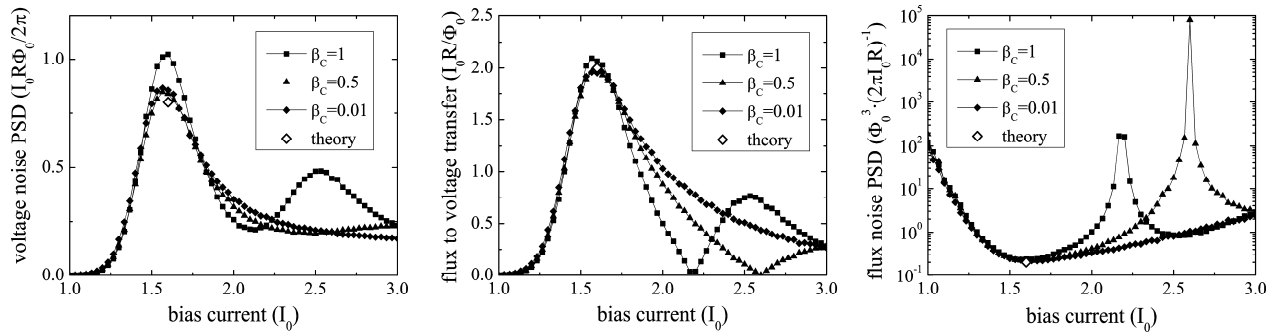

Fig. 3. A simulation is shown for three standard SQUIDs with differing β_C at one external flux $\Phi_e = 0.25 \cdot \Phi_0$ with changing bias current I. β_L was set to 1 and the noise parameter Γ was set to 0.05. The "theory" markers indicate values calculated from equations (3). See page 55 in reference [2] for comparison. Each working point was observed for 10^6 plasma oscillations. The σ of the excitation flux was $4 \cdot 10^{-4} \cdot \Phi_0$.

small-signal analysis, using the statistical independency of the excitation flux and SQUID noise, leads with (4) to

$$\partial V/\partial \Phi_e = \mathrm{cov}(V_{out}, \Phi_e) \cdot \mathrm{var}(\Phi_e)^{-1} \quad (5)$$

$$S_V = S_{V,out} - \mathrm{cov}(V_{out}, \Phi_e)^2 \cdot \mathrm{var}(\Phi_e)^{-1} \cdot (f_{LP} \cdot \pi/2)^{-1}. \quad (6)$$

S_Φ is then simply calculated via (1). In practice we use a Gaussian noise as excitation flux. The timescale of the change in excitation flux is chosen an order of magnitude slower compared to the output low-pass filter. The standard deviation σ of the excitation flux is typically chosen below one percent of a Φ_0 in order not to exceed the small-signal regime. We made sure that $S_{V,out}$ was at least an order of magnitude bigger than the artificially induced noise which is subtracted in (6).

For demonstration purposes, a simulation on a standard SQUID is shown in Fig. 3. The standard approximations (3) are well satisfied in the point of the best sensitivity.

Besides its flexibility, a big advantage of JSIM is speed: the sensitivity simulation on the extended model in section V included in total 10^9 plasma oscillations and took 12 hours on a Pentium 4 with 3 GHz.

IV. Modeling SQUIDs with Integrated Coils

The input coil is integrated on a widely used washer structure [18]. In references [8],[9] a model to determine the impedance of the washer at typical operation frequencies of the SQUID is presented alongside with an experimental verification. The model can be described by the left schematic in Fig. 4. The N turns of the coil are represented by N micro strip lines (MSLs) on top of the washer. The return current of each turn is directly induced in the washer, passing the hole inductance of the washer L_H and its slit inductance L_{SL}. This model resembles the interaction of washer and coil over the whole frequency range of interest.

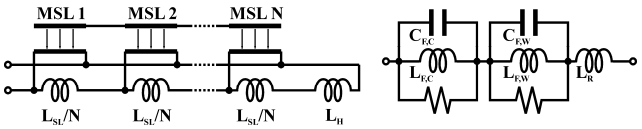

Fig. 4. Schematics for determining the impedance of a washer with integrated input coil. The left is the complete model from references [8],[9] and the right is our used lumped circuit element model for fitting the two fundamental resonances and a remaining inductance.

In Fig. 5, a calculation based on this model is shown as a solid line. The impedance corresponding to the dc SQUID inductance $2\pi \cdot f \cdot (L_H + L_{SL})$ can still be seen at the lowest depicted frequencies. When the frequency is close to the resonance frequency of the coil, where the wavelength roughly corresponds to the double of the length of the coil, the washer impedance is deviating from the dc inductance. The so-called *coil resonance* is reached. As can be seen in the middle part of Fig. 5, the effective inductance is much smaller at frequencies above this resonance compared to the dc case – roughly $L_{SL}/3$ [19]. If the hole inductance is much bigger than the slit inductance, the change can be tremendous. To determine L_H, we used the well-known formulas from reference [18]. For estimating the slit inductance L_{SL} we used numerical field calculation [20].

At even higher frequencies another typical resonance, the *washer resonance*, is reached. In this case, the dimensions of the area covered by the coil are of importance [19].

The complete model can directly be integrated in a SQUID model and solved by a circuit simulator [9] but this process is complex and time consuming, especially for SQUIDs with many integrated windings. One would need a network of N MSLs and N+1 inductances for one washer. In case of the SQUID presented in section V one signal coil has 60 turns. Using the complete model would extremely extend the simulation time, especially for a simulation on the sensitivity.

Accordingly, we decided to model the frequency dependent impedance as shown in the right schematic of Fig. 4 by a simplified model using two lumped circuit element resonance circuits for the coil- and the washer-resonance. Another inductance in series L_R qualitatively models the inductance above the washer resonance frequency. The elements of the simplified model were determined by fitting the calculations of the complete model. The parallel resistors set the quality factor $Q_{res} = R_{res} \cdot (C_{res}/L_{res})^{1/2}$ of the corresponding resonance.

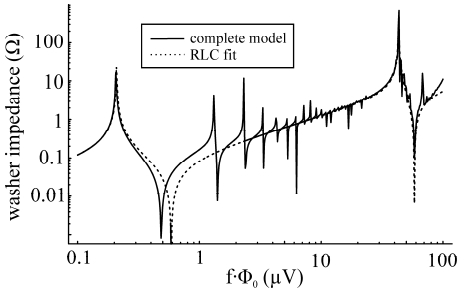

Fig. 5. The impedance of a washer with integrated coil versus the frequency. We multiplied the frequency with Φ_0 to make a comparison to the SQUID operation frequency possible, which is related to the measured dc voltage in the same way. The solid line shows the complete model calculation, where an open coil floating on the washer is assumed. The quality factor of the MSL was set to 1000. The dashed line is the lumped circuit element fit. The calculation corresponds to the signal washer of the SQUID investigated in section V, yielding the following elements for the lumped model: $L_{SIG,C}$=276 pH and $C_{SIG,C}$=9 nF for the coil resonance, $L_{SIG,W}$=18 pH and $C_{SIG,W}$=3.2 pF for the washer resonance and 22 pH remaining inductance.

On the one hand, with the lumped circuit elements, the interaction with circuits connected to the input coil can not be modeled anymore and the higher harmonics of the fundamental resonances are not included. On the other hand, the low computation time and the easy studying of effects of particular resonances, by changing parameters and testing their effect on the behavior of the complete SQUID, convinced us to follow this simplified approach.

V. Optimization of a DC SQUID with Integrated Coils

A. Fabrication technology

Our SQUID designs were fabricated at the IPHT Jena using the "LTS SQUID" process [14].

At the actual design step we used an aimed critical current density of 120 A/cm². The layer of the shunt resistors is made in *PdAu*, which stays normal conducting at temperatures typically reachable by a dilution refrigerator.

There are two Niobium layers available and the width and spacing inside the coils is 3 μm. Together with the 800 nm

thick insulating layer in *SiO* with a permittivity of 6.5, we could calculate [21] the distributed inductance and capacitance of the coil MSL to be $2.45 \cdot 10^{-7}$ H/m and $3.60 \cdot 10^{-10}$ F/m, respectively.

B. Summary of the design process

The most important discovery, while experimentally and numerically characterizing our old designs [12],[13], was an hysteresis originating from the coil resonance. A measurement of the phenomenon on another SQUID design is shown in Fig. 6. The hysteresis is usually not visible at a temperature of 4 K but still permits a low-noise operation in an eventually big lower voltage range [13]. This effect has been observed in numerical simulations before [5]-[7]. It originates from the change in effective inductance of the washer above the coil resonance frequency, as mentioned in the last section. For the SQUID whose characteristics are shown in Fig. 6 the effective inductance, as seen by the Josephson junctions, is halving its value while switching from the superconducting state to the voltage state. This results in an immediately changing working point. The resulting hysteretic voltage step is a function of Φ_e, β_L and the change in inductance between the superconducting (dc) state and the voltage (rf) state. Note that the typically used design approximation for the optimum operation voltage of the SQUID of $\approx 0.3 \cdot I_0 \cdot R$ [2] can easily be violated.

A damping resistance R_W connected across the SQUID inductance makes the characteristics steeper and helps to reduce the influence of resonances. If the size of this resistance is chosen similar to the shunt resistance R of the Josephson junction, the sensitivity can improve especially for high values of β_L [22]. For much smaller values of this damping resistor, similar hysteretic effects can occur even for SQUIDs without integrated coil [23].

Nevertheless, we believe that additional noise originating from the mentioned hysteretic voltage range can not be suppressed by damping resistors shunting the SQUID inductance or the input coil [11] down to our aimed operation temperatures. The effect has to be taken into account while choosing the operation frequency of an optimized design.

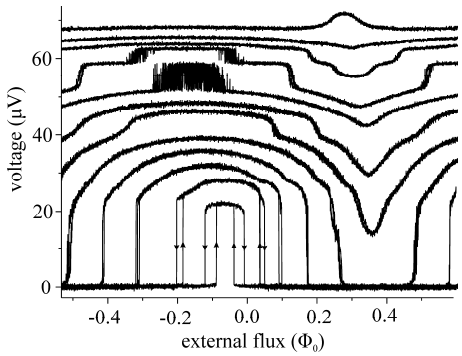

Fig. 6. Measured Φ_e-V characteristics of a SQUID with integrated flux transformer at a temperature of 0.1 K. The applied bias currents are 17, 18, 20, 22, 23, 25, 27, 29, 30, 33, 33 and 35 μA. Taken from reference [13].

Furthermore, in our last designs we could also identify the washer resonance point and other features introduced by shielded slits or other capacitances [13].

In conclusion, for the new design step we first minimized the coupled energy resolution as introduced in (2) on the basis of the standard approximations from (3). Here, we included estimations of parasitic inductances and the layout of the washers. At the same time, we tried to minimize the area of the integrated coil. Then we derived the model of the washer as shown before and included it in a complete SQUID model.

On basis of simulations on the sensitivity we then chose a working range by changing the value of the shunt resistors. The optimum operation range was set between the hysteretic range and the washer resonance. In combination with big area coils and thus low washer resonance frequency, this typically results in an over-damping $\beta_C \ll 1$ of the Josephson junction.

To allow a better cooling, we chose to use shunt resistors of a bigger size and electrically negligible cooling extensions [24]. The volume of the shunt resistor of the SQUID described in section V is $60 \cdot 50 \cdot 0.1$ μm^3 without the cooling fin.

VI. Characterization of a SQUID in Experiment and Simulation

A. Description of the SQUID design

For the utilization of the high-Q load [3] in FLL operation, especially a low direct parasitic inductance between the feedback- and the input coil is required [25],[26]. For that reason we made an adaption of a *Quantum Design* layout having a highly symmetric and gradiometric layout [4],[27]. As shown in Fig. 7, the design consists of two identical branches in parallel to the Josephson junctions. Those two branches consist of a series connection of one signal- and one feedback-washer with integrated coils. We added two resistors to split the bias currents in a balanced way into the parallel branches to minimize a parasitic external flux caused by the bias current. As mentioned before, a washer damping resistor of the same size as the shunt resistor is integrated.

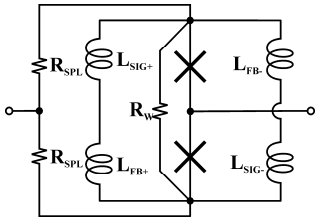

Fig. 7. Schematic of the washer configuration of the dc SQUID with a parallel washer configuration. It consists of four washers, two gradiometric washers with an integrated signal coil and two gradiometric washers with an integrated feedback coil.

The impedance of the washer with integrated signal coil with N=60 can be seen in Fig. 5. For the washer with the 3 feedback windings we only modeled the coil resonance. The resulting simulation model is shown in Fig. 8. Here, the two parallel branches were summarized in one branch. Because of the low resonance frequency of the coil resonance we reduced its Q to 1 to accelerate changes of energy stored in the inductor and save simulation time, which is crucial for a complete noise characterization. For the other resonances we chose a guessed value of Q=1000. Parasitic inductances originating from MSLs and crossing of slits (L_{P1},L_{P2}) were added in series with the Josephson junctions and in series to the washer damping resistance R_W. The effective slit

inductances of the connection of washers were added in series to the remaining inductance of the models of the washers in L_{P4}. The values of those parasitic inductances and the one in series with the bias splitting resistors L_{P3} were estimated via numerical inductance calculation on simplified geometries [20].

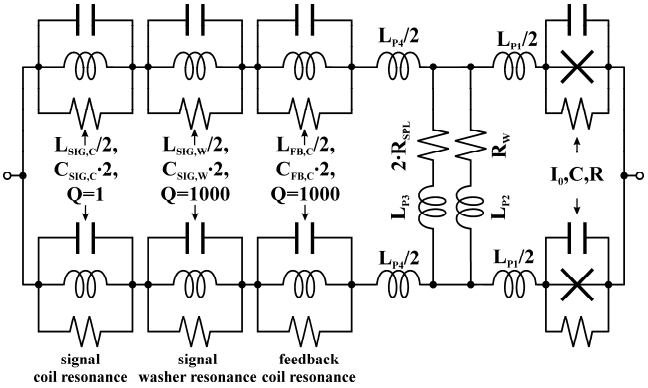

Fig. 8. Schematic of the simulation model of the dc SQUID with a parallel washer configuration. Noise sources, not shown here for simplicity, are only attached to the shunt resistors R, to the washer damping resistor R_W and the bias splitting resistors R_{SPL}, but not to the damping resistors of the resonators, which only set the given Q of each resonance. $L_{SIG,C}$=276 pH/2, $C_{SIG,C}$=9 nF·2, $L_{SIG,W}$=18 pH/2, $C_{SIG,W}$=3.2 pF·2, $L_{FB,C}$=36 pH/2, $C_{SIG,C}$=0.63 pF·2, L_{P1}=20 pH, L_{P2}=20 pH, L_{P3}=350 pH, L_{P4}=49 pH, C=0.77 pF. The factors or fractions of 2 for the resonance fits emphasize that here two parallel branches are modeled in one SQUID loop, see Fig. 7. Used experimental values are I_0=18 μA, R_W=3.2 Ω, R_{SPL}=1.3 Ω. See text for details.

With a design value of the critical current of $I_{0,D}$=13 μA and the estimated SQUID inductance of 230 pH the screening parameter $\beta_{L,D}$ yields 2.9. The estimated effective SQUID inductance in the voltage state was estimated to be about 40 % of its dc value. This originates, as shown before, in the coil resonance of the signal washer with 60 windings. The value of the shunt resistor was chosen on basis of the simulation to R_D=3.6 Ω, leaving a margin between the hysteretic voltage range and the washer resonance of about $0.5 \cdot I_{0,D} \cdot R_D$.

To include the capacitance introduced by the big shunt resistor, we used a rule-of-thumb from reference [2] and added half of its value to the junction capacitance. The McCumber parameter yields $\beta_{C,D}$=0.3.

For the two input coils connected in series, we estimated a mutual inductance M_D of 15 nH and an inductance $L_{IN,D}$ of 1.6 μH. The simulated flux noise of the SQUID was 1.7 $\mu\Phi_0/\sqrt{\text{Hz}}$ at a temperature of 4.2 K, yielding with (2) a coupled energy resolution of 420 ħ.

B. Description of the characterization process

We characterized the fabricated samples in a ^{4}He bath. The SQUIDs had a higher critical current compared to the design value. From I-V measurements, we estimated a critical current I_0=18 μA. The value of the shunt resistors was derived from the high voltage region to R=3.2 Ω, so the $I_0 \cdot R$ product reached a 25% higher value compared to the design aim and β_L increased by 40% to a value of 4.1. The value of the two bias splitting resistors in parallel was derived from the superconducting part of the SQUID to $R_{SPL}/2$=0.66 Ω. In following graphs we compensated for this resistor, because the additional dc voltage has no influence on the performance of the SQUID. Nevertheless, its noise and possible damping properties are included, as can be seen in Fig. 8.

We measured a mutual inductance between the SQUID and the integrated signal coils of M=13 nH. By shorting the input coil with a resistor in the order of 10 mΩ and measuring its, via the coil low-pass filtered, noise spectrum in FLL, we could estimate the input coil inductance to L_{IN}=1.5 μH. This is possible because of the low parasitic coupling between the feedback and the signal coil systems. With a normal SQUID design, the in such a way determined inductance usually takes lower values than the real inductance. Both M and L_{IN} are in good agreement with the design values.

During the experiments, we did not connect any R-C shunt connected to the input coil [11], because we believe this only allows to reach lower noise levels in the hysteretic voltage ranges. Here, excess noise should cause an irregular temperature dependence. We placed the sensor as the first stage in a two-stage SQUID setup [2] and used a dc SQUID with flux transformer with a mutual inductance of 7 nH as the second stage. The first stage was voltage biased with a resistor of 0.5 Ω. To reduce negative effects of wideband noise in the second stage, we placed a 50 μH inductance as a filter between the first and the second stage. This way, we reached a stable operation of the SQUID system with a high small signal flux gain between the first and second stage of the order of 50. This eliminates a noise contribution of the room temperature amplifier completely. In FLL, we reached typical bandwidths of about 50 kHz with this setup. We were also able to directly measure the voltage across the bias resistor of the first stage. With the known bias current, the voltage and current working point of the first stage SQUID can be calculated. Again, we subtracted the voltage across the series splitting resistor.

We performed a detailed noise characterization by biasing the first stage at differing currents and searching for a low flux noise over the, due to the high flux gain, multiple possible locking points. Besides measured flux noise values, we recorded the corresponding voltage of the SQUID.

Later, the temperature was reduced to 1.5 K by reduction of the pressure of the ^{4}He bath. At the point of best sensitivity we found a white flux noise $S_\Phi^{1/2}$ of 2.0 $\mu\Phi_0/\sqrt{\text{Hz}}$ and 1.2 $\mu\Phi_0/\sqrt{\text{Hz}}$ over a frequency range of about 10 Hz to 10 kHz at a temperature of 4.2 K and 1.5 K, respectively. With (2), this corresponds to a coupled energy resolution ε of 700 ħ at 4.2 K and 250 ħ at 1.5 K. The noise referred to the input current $S_\Phi^{1/2}/M$ is 320 $\text{fA}/\sqrt{\text{Hz}}$ at 4.2 K or 190 $\text{fA}/\sqrt{\text{Hz}}$ at 1.5 K.

The linear scaling of the flux noise PSD with temperature indicates that the noise is determined by the noise in the damping resistors of the SQUID.

C. Summary of the results of the measurement in comparison with the simulations

We adapted our originally made model to the measured values of the critical current of the Josephson junctions and the resistors, as already shown in Fig. 8.

The agreement between measured and simulated Φ_e-V characteristics is very good, as can be seen in Fig. 9. The minimum measured critical current of the SQUID of 28 μA is reproduced by the simulation. The same value was also

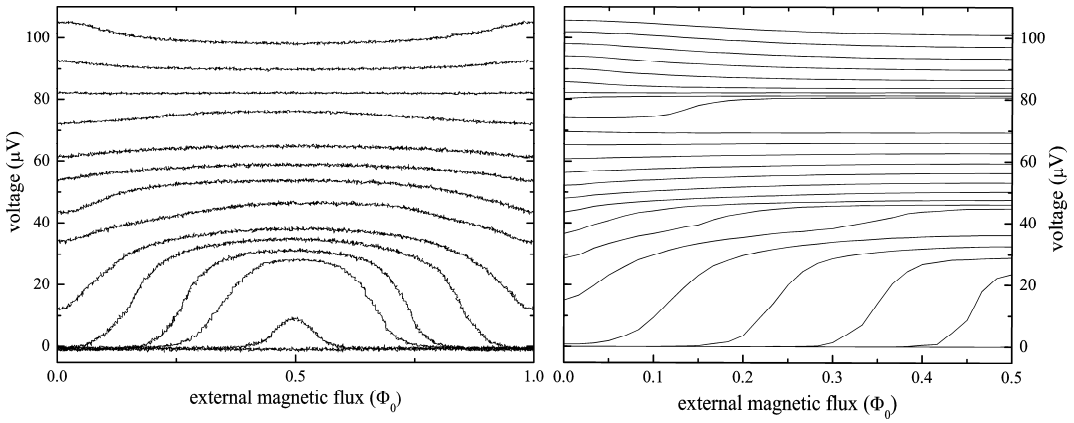

Fig. 9. Φ_e-V characteristics at a temperature of 4.2 K. Left: Measured characteristics at differing bias currents I=0 (superconducting), 28, 30, 32, 34, 36, 40, 44, 48, 52, 57, 62, 67, 72 μA. From the measured voltage we subtracted the voltage over the bias splitting resistors of $R_{SPL}/2 \cdot I$=0.66 Ω·I. The dc external magnetic flux was subtracted. Right: Simulation of the model shown in Fig. 8 at differing bias currents I=26 (superconducting) till 72 μA in steps of 2 μA. Each working point was observed for 20 μs (10^6 plasma oscillations) with a low-pass cutoff frequency of 10 MHz. No excitation flux was applied.

estimated from I-V measurements. The good fit indicates that the β_L of 4.1, calculated from the measured critical current and the modeled inductances, seems to be correct. The measurement shows slightly asymmetric characteristics, which we address to an asymmetry in the layout of the washer damping resistor.

To investigate the origin of some features, we performed some test simulations by changing several elements in the model. The lower voltage region is again quite steep due to the, here smeared out, hysteresis originating from the coil resonance of the signal washers and due to the connected washer damping resistor. Furthermore, a small irregularity in the range of 40 μV can be seen which is caused by the washer resonance of the signal washer. The voltage step around 75 μV is due to the coil resonance of the feedback washer.

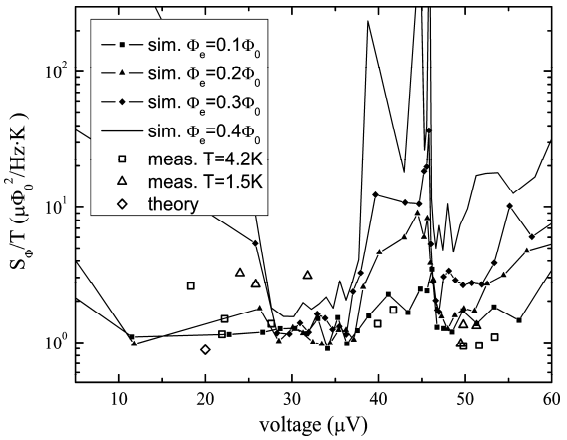

Fig. 10. Simulated flux noise PSD S_Φ at T=4.2 K and measured values at T=4.2 K and 1.5 K. The "theory" marker is the value calculated from (3). The simulations were done on the model shown in Fig. 8. Here, each working point was observed for 0.2 ms ($8 \cdot 10^6$ plasma oscillations) with a low-pass cutoff frequency of 10 MHz and a σ of the excitation flux of $4 \cdot 10^{-3}$ Φ_0. The measurements were done in a 2-stage SQUID setup. Note the influence of the washer resonance of the signal washer ($L_{SIG,W}$-$C_{SIG,W}$) around 40 μV.

In Fig. 10, the measured and simulated flux noise PSD S_Φ are shown. As described before, the voltage in the experiment was also estimated for each noise measurement. As one can see, the voltage range of the best measured sensitivity at a voltage of 50 μV is just above the washer resonance of the signal washer, in contrary to the originally planned operation below the resonance. The reason is the spread during the fabrication. Please note that the minimum noise in the simulation is at low values of external flux, which we could also verify in the experiments. Within the named resonance, the noise in the simulation is increased and also in the measurement we were not able to reach a good sensitivity. Although the point is hard to spot in the characteristics, its degrading influence on the sensitivity is clear. Low noise working points just below the resonance seen in the simulation could not be observed in the measurement. Please note that at even lower voltages we reached a good noise at 4.2 K, but this noise did not scale well with temperature. We address this to the hysteresis described before.

In comparison, although the noise levels at the exact voltages do not fit completely, the agreement between the measurement and the simulation is remarkable.

VII. Conclusion and Outlook

Using the SPICE-based simulator JSIM, we developed a feasible system for numerical characterization of dc SQUIDs. Due to its speed and flexibility, also complex circuit models can be evaluated. This system was then used to optimize the operation frequency of the design of a SQUID with an integrated input coil of 1.5 μH. The expected coupled energy resolution was 420 ħ at 4.2 K.

Despite the variation during the fabrication, we measured a good coupled energy resolution of 700 ħ at 4.2 K, which scaled down linearly to 250 ħ at 1.5 K. A good agreement in the characteristics and the noise between the real-world and the numerical experiment is shown.

Due to the big size of the shunt resistors, we expect a minimum additional coupled energy resolution of about 50 ħ in a dilution refrigerator, which is about the same value achieved in [4]. This will be part of further investigations.

References

[1] C. D. Tesche, and J. Clarke, "DC SQUID: Noise and optimization," *J. Low Temp. Phys*., vol. 29, pp. 301-331, Nov. 1977; J. J. P. Bruines, V. J. de Waal and J. E. Mooij, "Comment on 'DC SQUID: Noise and optimization' by Tesche and Clarke," *J. Low Temp. Phys*., vol. 46, pp. 383-386, Feb. 1982.

[2] J. Clarke, and A. I. Braginski, Ed. *The SQUID handbook Vol. 1*, Weinheim, Germany: Wiley-VCH, 2004.

[3] A. de Waard, L. Gottardi, J. Van Houwelingen, A. Shumack, and G. Frossati, "MiniGRAIL, the first spherical detector," *Class. Quantum Grav.*, vol. 20, pp. S143-S151, Apr. 2003.

[4] P. Falferi et al., "27 h-bar SQUID amplifier operating with high-Q resonant input load," *Appl. Phys. Lett*., vol. 88, pp. 062505-3, Feb. 2006.

[5] C. D. Tesche, "Analysis of a double-loop dc SQUID," *J. Low Temp. Phys.*, vol. 47, pp. 385-410, Jun. 1982.

[6] D. Drung, and W. Jutzi, "Hysteretic noise simulation of dc SQUIDs with input coil" in *Superconducting Quantum Interference Devices and their Applications*, H. D. Hahlbohm, H. Luebbig, Ed. Berlin, New York: Walter de Gruyter p. 807, 1985

[7] T. Ryhänen, and H. Seppä, "Effect of parasitic capacitance and inductance on the dynamics and noise of dc superconducting quantum interference devices," *J. Appl. Phys*., vol. 71, pp. 6150-6166, Jun. 1992.

[8] K. Enpuku, R. Cantor, and H. Koch, "Modeling the direct current superconducting quantum interference device coupled to the multiturn input coil. II," *J. Appl. Phys.*, vol. 71, pp. 2338-2346, Mar. 1992.

[9] G. Hildebrandt, F. H. Uhlmann, G. M. Daalmans, and F. R. Bommel, "A novel approach in calculating V-I curves of a DC-SQUID coupled to a planar input coil," *IEEE Trans. Appl. Supercond.*, vol. 6, pp. 19-23, 1996.

[10] J. Schambach, H. G. Meyer, L. Warzemann, P. Weber, K. Blüthner, G. M. Daalmans, F. Bömmel, and D. Uhl, "Analytical calculation of the I - V characteristics of SQUIDs with parasitic elements," *Supercond. Sci. Technol.*, vol. 9, pp. 617-621, 1996.

[11] J. Knuutila, A. Ahonen, and C. Tesche, "Effects on DC SQUID characteristics of damping of input coil resonances," *J. Low Temp. Phys.*, vol. 68, pp. 269-284, 1987.

[12] J. Pleikies, O. Usenko. K. H. Kuit, J. Flokstra, A. de Waard, and G. Frossati, "SQUID Developments for the Gravitational Wave Antenna MiniGRAIL," *IEEE Trans. Appl. Supercond.*, vol. 17, pp. 764-767, 2007.

[13] J. Pleikies, O. Usenko, and J. Flokstra, "Numerical studies on dc-SQUID sensors with tightly coupled input coil*," J. Phys.: Conf. Ser.*, vol. 97, p. 012254, 2008.

[14] IPHT Jena e.V., Department of Quantum Electronics, Winzerlaer Str. 10, 07745 Jena, Germany. LTS SQUID process, LTS SQUID technology design rules online available: http://www.ipht-jena.de/uploads/media/a13_ipht_squid_1_4_04.pdf, Aug. 2008.

[15] J. Clarke, C.D. Tesche, and R.P. Giffard, "Optimization of dc SQUID voltmeter and magnetometer circuits," *J. Low Temp. Phys.*, vol. 37, pp. 405-420, Nov. 1979.

[16] E. S. Fang, and T. van Duzer, „A Josephson integrated circuit simulator (JSIM) for superconductive electronics application," Ext. abstr. *2nd International Superconductivity Electronics Conference*, Tokyo, pp. 407-410, June 1989.

[17] J. Satchell, "Stochastic simulation of SFQ logic," *IEEE Trans. Appl. Supercond.,* vol. 7, pp. 3315-3318, 1997.

[18] J. Jaycox and M. Ketchen, "Planar coupling scheme for ultra low noise DC SQUIDs," *IEEE Trans. Magn.*, vol. 17, pp. 400-403, 1981.

[19] K. Enpuku, R, Cantor, and H. Koch, "Modeling the dc superconducting quantum interference device coupled to the multiturn input coil. III," *J. Appl. Phys.*, vol. 72, pp. 1000-1006, Aug. 1992.

[20] Inductance extraction software: FastHenry 3.0wr, Whiteley Research Inc., 456 Flora Vista Avenue Sunnyvale, CA 94086, U.S.A., Available online: http://www.srware.com.

[21] W.H. Chang, "The inductance of a superconducting strip transmission line," *J. Appl. Phys.*, vol. 50, pp. 8129-8134, Dec. 1979.

[22] K. Enpuku, K. Yoshida, and S. Kohjiro, "Noise characteristics of a dc SQUID with a resistively shunted inductance. II. Optimum damping," *J. Appl. Phys.,* vol. 60, pp. 4218-4223, Dec. 1986.

[23] I. L. Atkin, E. Abraham, and C. M. Pegrum, "Voltage-flux bistability in damped direct current SQUIDs," *Appl. Phys. Lett*., vol. 69, pp. 1309-1311, 1996.

[24] F.C. Wellstood, C. Urbina, and J. Clarke, "Hot-electron effects in metals," *Phys. Rev. B*, vol. 49, pp. 5942-5955, Mar. 1994.

[25] W.M. Folkner, M. V. Moody, J. P. Richard, K. R. Carroll, and C. D. Tesche, "Instrumentation of a resonant gravitational radiation detector with a planar thin-film dc SQUID," *J. Appl. Phys.,* vol. 65, pp. 5190-5196, Jun. 1989.

[26] Vinante, M. Bonaldi, P. Falferi, M. Cerdonio, R. Mezzena, G. A. Prodi, and S. Vitale, " Stabilization and optimization of a two-stage dc SQUID coupled to a high Q resonator," *Physica C*, vol. 368, pp. 176-180, Mar. 2002.

[27] M. B. Simmonds, "High symmetric dc SQUID system," U.S. Patent 5053834, 1991.